Optics Communications 289 (2013) 53–59

Contents lists available at SciVerse ScienceDirect

Optics Communications

journal homepage: www.elsevier.com/locate/optcom

Integrated optical add-drop multiplexer based on a compact parent-sub microring-resonator structure

Hai Yan, Xue Feng*, Dengke Zhang, Yidong Huang

State Key Laboratory of Integrated Optoelectronics, Department of Electronic Engineering, Tsinghua University, Beijing 100084, China

ARTICLE INFO

Article history:
Received 10 July 2012
Received in revised form
21 September 2012
Accepted 23 September 2012
Available online 11 October 2012

Keywords:
Optical add-drop multiplexer
Series-coupled microring resonators
Vernier effect

ABSTRACT

A compact parent-sub microring-resonator structure for highly integrated optical add-drop multiplexer (OADM) is proposed and demonstrated by numerical simulation. Due to Vernier effect, large FSR can be obtained by cascaded microrings with relatively large diameter. Furthermore, nearly uniform channel spacing is achieved due to employment of multiple resonances of the parent ring. As a representative example, a 4-channel OADM is simulated. Box-like response with flat passband is obtained by optimizing coupling coefficients. Add-drop crosstalk of -15 dB, drop loss of near 0 dB, and adjacent channel crosstalk of -25 dB can be observed from the calculated transmission spectra. The reconfigurability, loss tolerance as well as the relation between bandwidth and crosstalk are also discussed.

1. Introduction

On-chip optical interconnect offers a promising way to greatly enhance the performance of future computer systems due to its ability of high data transmission rate and low power consumption [1,2]. To improve the integration density of such on-chip optical networks, wavelength division multiplexing (WDM) is a natural solution [3]. One of the key components in a WDM transmission link is optical add-drop multiplexer (OADM), which allows flexible addition and extraction of WDM signals. Microring resonator based add-drop filter has been widely investigated as a candidate for highly-integrated OADM [4–8]. However, it is challenging to achieve large free spectral range (FSR). The most direct solution is to reduce the radius of the microring. In [8–10], FSR as wide as 32 nm, 52 nm and 62.5 nm have been experimentally demonstrated with a microring radius of only 2.5 μm or 1.5 μm. A widely reported alternative to extend the FSR is utilizing the Vernier effect by coupling microring resonators of different radii in series [11–13]. A third approach to increase the FSR is combining the microring resonator with photonic bandgap structures to remove non-desired resonances [14].

The scheme using the extremely small microring achieves minimum footprint as well as large FSR that covers the span of C-band. However, such small bending radius inevitably leads to nontrivial loss so that special optimization in both design and fabrication is needed. The second scheme deploying the Vernier effect could achieve large FSR with large rings (radius >5 μm, the bending loss could be neglected). Nonetheless, its footprint is larger and scales up with the number of channels in multi-channel applications. The channel spacing between adjacent add-drop filters is also hard to keep uniform. In the third scheme mentioned above, though a very wide FSR of over 140 nm is theoretically obtained, other performance parameters such as insertion loss and through port extinction are compromised.

In this paper, we propose a parent-sub microring structure for OADM which consists of a parent ring and several sub rings coupled to the parent one. This compact structure takes advantage of the Vernier effect to obtain a large FSR with relatively large microrings (24 nm FSR with ring radius >8 μm is obtained as shown in Section 3). The usual Vernier arrangement combines a larger ring and a smaller ring to an add-drop filter and then put several such filters in tandem to construct an OADM. Comparing to this arrangement, our setup is quite different, where all the larger rings are merged into a single parent ring and the smaller rings are put around the parent one. Therefore a smaller size as well as uniform channel spacing could be obtained since multiple resonances of the same ring (parent ring) are adopted. With optimized coupling coefficients, box-like response with flat passband is achieved. Furthermore, the reconfigurability, fabrication tolerance as well as the tradeoff between bandwidth and crosstalk are discussed.

2. Design overview and analysis

In this section, we will introduce the compact microring OADM structure and its operating principle. Then detailed analysis is presented.

* Corresponding author. Tel.: +86 10 62797073/803; fax: +86 10 62797073/807.
E-mail address: x-feng@tsinghua.edu.cn (X. Feng).

0030-4018/$ - see front matter © 2012 Elsevier B.V. All rights reserved.
http://dx.doi.org/10.1016/j.optcom.2012.09.059

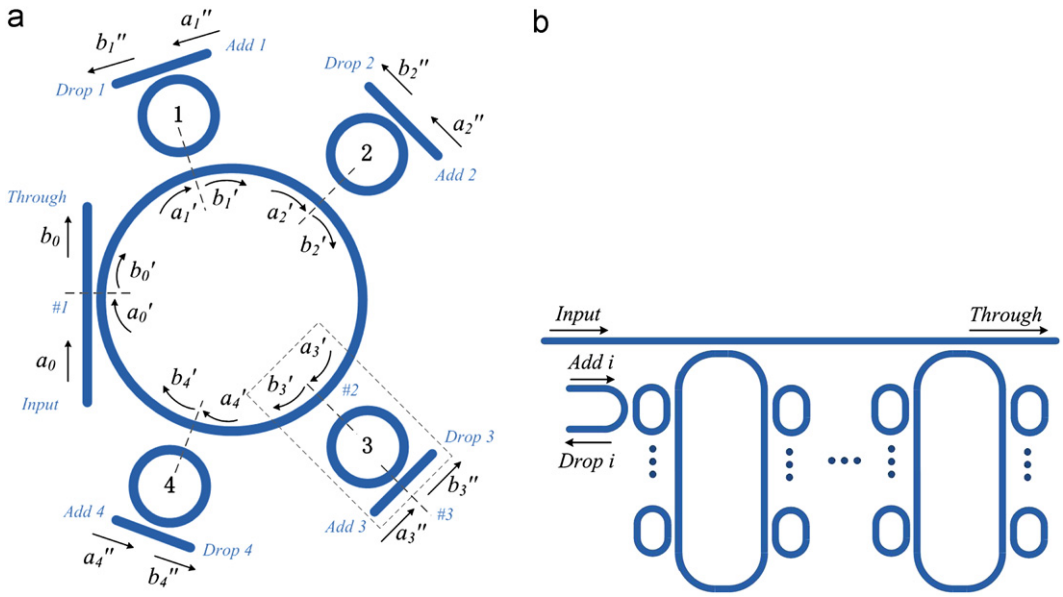

Fig. 1. Schematic of the proposed parent-sub microring-resonator structure (a) and cascading scheme for more WDM channels (b).

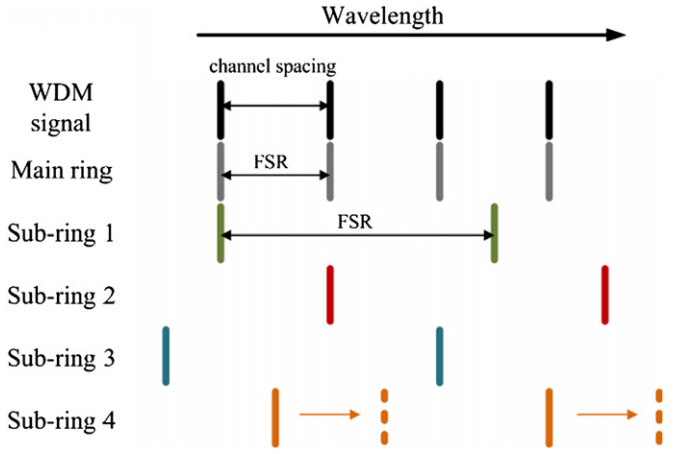

Fig. 2. Schematic of the wavelength relation between the WDM channels and the microring resonances.

The schematic of the proposed OADM is shown in Fig. 1. There is a parent ring with several sub-rings independently coupled to it. Here, a special case of four sub-rings is illustrated. The bus waveguides are side-coupled to each of the rings and serve as input and output ports.

To explain the operating principle, we suppose that there are 4 channels of WDM signals injected at the input port. The central wavelength of each channel and the resonant wavelengths of the ring resonators are illustrated as the vertical bars in Fig. 2. The free spectral range (FSR) of the parent ring is equal to the channel spacing and its resonant wavelengths match the four WDM channels. The FSR of the sub-ring is much wider (2.5 times of the channel spacing in this case) so that only one resonance of the parent ring could be matched at a time. Four channels would output from the four drop ports (drop m in Fig. 1(a), $m=1, 2, 3, 4$) after passing through the parent ring and one of the sub-rings. By tuning the resonance of the sub-ring away from that of the parent ring (shown in Fig. 2 as dashed bars), the corresponding channel would be blocked by the sub-ring and output from the through port. In this way, each channel can be selectively dropped.

Similarly, for case of "adding channels", we assume that such four channels are incident at the add ports. If the resonance of the sub-ring and parent ring are matched, they could pass through a sub-ring, the parent ring, and then be added to the through port. Otherwise, the channel would not be added. Then selective adding of the channels could also be achieved.

In principle, more sub-rings could be used to increase the number of WDM channels. However, due to the practically limited circumference of the parent ring, the number of the sub-rings is limited. To achieve even more channels, cascading the proposed parent-sub ring structures in series is a solution (see Fig. 1(b)). For example, using two such structures each with n sub-rings, one for odd channels and the other for even channels, an OADM for $2n$ channels could be constructed.

The aforementioned process could be quantitatively described by transfer matrix method [15,16]. The involved electric field amplitudes are illustrated in Fig. 1(a). The transfer matrices are denoted as the following: P_1 for coupling region between bus waveguide and the parent ring (coupling region #1), P_{2m} for the coupling region between the parent ring and sub-ring m ($m=1, 2, 3, 4$) (coupling region #2), P_{3m} for the coupling region between sub-ring m and bus waveguide (coupling region #3); Q_{1m} and Q_{2m} for the propagation within the parent ring and sub-ring m. Then the field amplitude relation among all the input and output ports could be expressed as:

$$\begin{pmatrix} a_m'' \\ b_m'' \end{pmatrix} = P_{3m}Q_{2m}P_{2m}Q_{1m}P_1 \begin{pmatrix} a_0 \\ b_0 \end{pmatrix} \tag{1}$$

These transfer matrices, except Q_{1m}, can be easily expressed with parameters including coupling coefficients, roundtrip attenuation, and phase shift [15,16]. We suppose that:

$$\begin{pmatrix} a_m'' \\ b_m'' \end{pmatrix} = P_{3m}Q_{2m}P_{2m} \begin{pmatrix} a_m' \\ b_m' \end{pmatrix} = \begin{bmatrix} A_m & B_m \\ C_m & D_m \end{bmatrix} \begin{pmatrix} a_m' \\ b_m' \end{pmatrix} \tag{2}$$

$$\begin{pmatrix} a_0' \\ b_0' \end{pmatrix} = P_1 \begin{pmatrix} a_0 \\ b_0 \end{pmatrix} = \begin{bmatrix} A_0 & B_0 \\ C_0 & D_0 \end{bmatrix} \begin{pmatrix} a_0 \\ b_0 \end{pmatrix} \tag{3}$$

For Q_{1m}, we first get the relation between a_m' and b_m' from (2) where add port input is set to zero, i.e. $a_m''=0$:

$$\frac{b_m'}{a_m'} = -\frac{A_m}{B_m} = St_m \tag{4}$$

Then Q_{1m} can be expressed by the following equation:

$$\begin{pmatrix} a'_m \\ b'_m \end{pmatrix} = Q_{1m}\begin{pmatrix} a'_0 \\ b'_0 \end{pmatrix} = \begin{bmatrix} 0 & \mu_0^{l_m/L} e^{-i\beta l_m} \prod_{k=0}^{m-1} St_k \\ \left(\mu_0^{(L-l_m)/L} e^{-i\beta(L-l_m)} \prod_{k=m+1}^{5} St_k\right)^{-1} & 0 \end{bmatrix} \begin{pmatrix} a'_0 \\ b'_0 \end{pmatrix} \tag{5}$$

where μ_0 is the roundtrip amplitude transmission of parent ring and β is the propagation constant, l_m is the transmission length from b'_0 to a'_m and L is the circumference of the parent ring. We also suppose $St_0 = St_5 = 1$.

With (5), power transmission ratio for through port and drop ports could be obtained:

$$T_{through} = \left|\frac{b_0}{a_0}\right|^2 = \left(-\frac{A_0 - C_0\mu_0 e^{-i\beta L}\prod_{k=1}^{4} St_k}{B_0 - D_0\mu_0 e^{-i\beta L}\prod_{k=1}^{4} St_k}\right)^2 \tag{6}$$

$$T_{drop\_m} = \left|\frac{b''_m}{a_0}\right|^2 = \left(\mu_0^{l_m/L} e^{-i\beta l_m}(C_0 + D_0 T)\left(C_m - \frac{A_m D_m}{B_m}\right)\prod_{k=0}^{m-1} St_k\right)^2 \tag{7}$$

3. Simulation results

To demonstrate the performance of our proposed OADM structure, a four-channel device is designed and simulated following (6) and (7). The WDM signals are assumed around wavelength of $\lambda_0 = 1550$ nm with channel spacing of 4.8 nm and TE polarization. We consider the proposed structure fabricated on silicon-on-insulator (SOI) substrate. All the bus waveguides and microring resonators are using the same Si channel waveguide ($n_{Si} = 3.45$) with SiO_2 claddings ($n_{SiO2} = 1.46$). The width and height of the channel waveguide are 500 nm and 220 nm, respectively. The propagation loss is set as 0.2 dB/mm. Then the group index (n_g) of the waveguide around 1550 nm could be calculated as 3.84. According to Fig. 2, the FSR of the parent ring and sub-rings should be 4.8 nm and 12 nm (2.5 times of channel spacing), respectively. Then the FSR of the parent-sub ring structure should be 24 nm due to Vernier effect. With the equation $FSR = \lambda_0^2/n_g L$, the circumference of the rings are determined as $L_0 = 130.4$ μm and $L_{1-4} = 52.2$ μm (corresponding radius: $R_0 = 20.75$ μm, $R_{1-4} = 8.31$ μm).

Next, the coupling coefficients should be determined. For simplicity, the coupling condition for all the sub-rings are considered identical, *i.e.*, the transfer matrix P_{2m} (or P_{3m}) is the same for each m. Thus we can use self-coupling coefficients r_i ($i = 1, 2, 3$) and cross-coupling coefficients t_i ($i = 1, 2, 3$) to describe coupling region #i [15]. The coupling is considered lossless, so $r_i^2 + t_i^2 = 1$. To obtain a preferable result, we did some preliminary simulations and set $r_1 = 0.8700$, $r_3 = 0.8851$. If circular rings are adopted, the calculated gap distance is ~40 nm. However, by using racetrack ring resonators (see Fig. 1(b)), the corresponding gap distance is about 160 nm when the straight section of the coupling region is 5 μm. Considering the fabrication difficulty, the racetrack resonators are more suitable for practical devices. Since the coupling coefficients are firstly settled, the value of gap distance would not affect the following calculation and discussion. After r_1 and r_3 are settled, r_2 is determined by the optimum condition obtained in Appendix. This condition guarantees a flat passband in the drop port spectrum for an asymmetrical second-order series-coupled ring resonator filter. Since the whole structure in Fig. 1(a) can be approximately simplified to such a filter for any single channel, the optimum condition is applicable.

The calculated coupling coefficients are as follows:

$r_1 = 0.8700$, $r_2 = 0.9885$, $r_3 = 0.8851$

$t_1 = 0.4931$, $t_2 = 0.1515$, $t_3 = 0.4654$

The resonances of the sub-rings are slightly tuned to match that of the parent ring so that all four channels could be dropped. The calculated transmission spectrum of all the output ports is presented in Fig. 3. The central wavelengths of the four channels (*i.e.* the resonances of the parent ring) are 1542.3 nm, 1547.1 nm, 1551.9 nm, and 1556.7 nm. A nearly uniform channel spacing of 4.8 nm is obtained. For through port, the extinction around resonances is less than −15 dB. For drop port 1, drop loss for channel 1 ($\lambda = 1542.3$ nm) is near 0 dB. Thus the add-drop crosstalk (the difference between these two values) is lower than −15 dB. Here, the 3 dB bandwidth and shape factor (the ratio of 1 dB and 10 dB bandwidth) are 0.46 nm and 0.41, respectively. Furthermore, there is also crosstalk between channels due to interstitial peaks. For drop port 1, the crosstalk for adjacent channels is about −25 dB while that for non-adjacent channels is about −20 dB. For other drop ports, almost the same results can be observed.

In order to investigate the impact of changing a channel's operating state (from dropping to passing through), some further simulations are carried out. The results of two typical ones are shown in Fig. 4. In Fig. 4(a), the status of channel 1 ($\lambda = 1542.3$ nm) is varied from dropping to passing through by

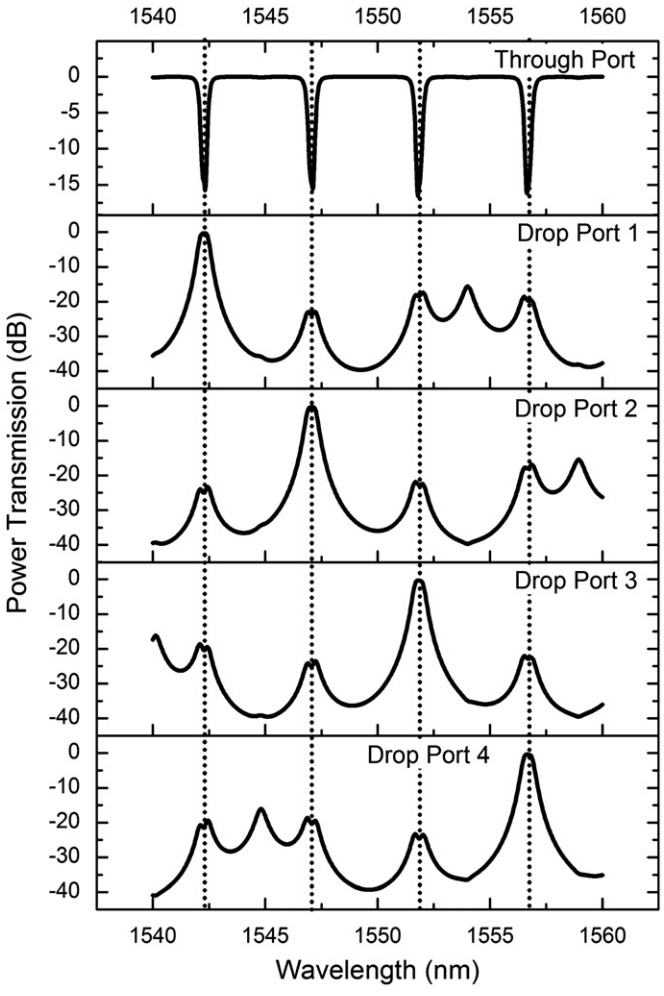

Fig. 3. Simulated transmission spectra of the proposed OADM when all four channels are dropped.

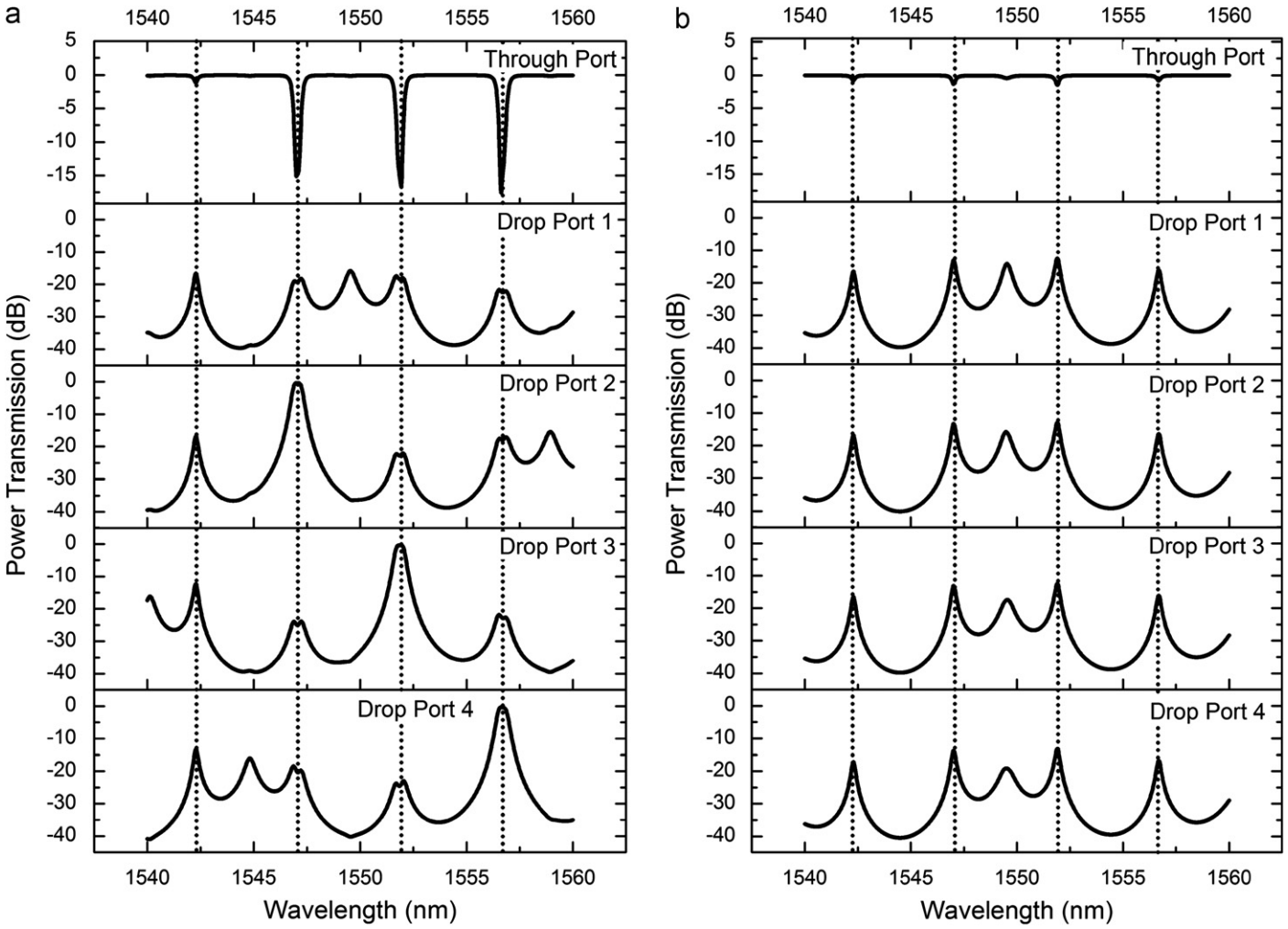

Fig. 4. Simulated transmission spectra of the proposed OADM when (a) channel 1 is tuned from dropping to passing through and (b) all four channels are tuned to passing through.

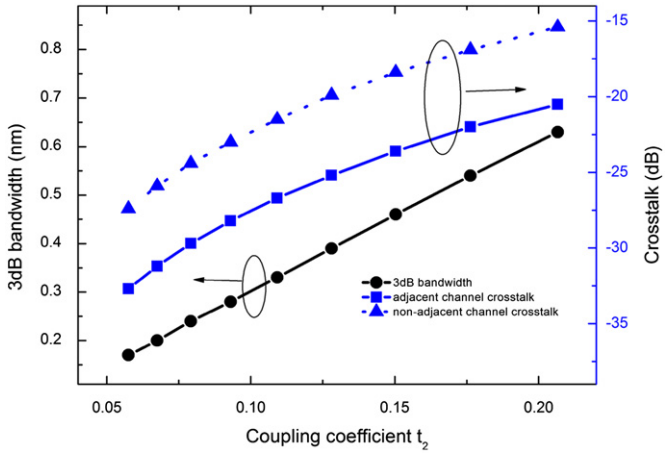

Fig. 5. Simulated 3-dB bandwidth and channel crosstalk as a function of coupling coefficient t_2.

changing the refractive index of sub-ring 1 ($\Delta n=0.011$) so that the resonant wavelength is tuned to the middle of the second ($\lambda=1547.1$ nm) and third channel ($\lambda=1551.9$ nm). Now the through port extinction for channel 1 is only -1 dB and drop port loss reduces to less than -15 dB at drop port 1. For other channels, the add-drop crosstalk and 3 dB bandwidth remain nearly unchanged. However, more signal power of channel 1 output from drop port 2, 3, 4 so that the crosstalk would be deteriorated to $-10\sim-15$ dB. In Fig. 4 (b), the case of all WDM channels passing through are presented. All the WDM signals pass through the device with 1–2 dB insertion loss and the drop port transmission is less than -10 dB.

Table 1
Typical spectrum parameters for different propagation loss values.

Propagation loss (dB/mm)	Through port extinction (dB)	Drop loss (dB)	3 dB bandwidth (nm)	Adjacent channel crosstalk (dB)
0.2	−16	−0.3	0.46	−23.6
1	−14.5	−0.8	0.46	−23.7
2	−13.5	−1.4	0.46	−23.9

In practice, the refractive index change can be achieved through the thermo-optic effect (TOE) or free-carrier effect (FCE). In our case, the index change is as large as $\Delta n=0.011$. If the FCE is adopted, additional absorption loss of about 25 dB/mm would be introduced [17], so that FCE is not a practical solution. The TOE could induce large refractive index change ($dn/dT\approx 1.86\times10^{-4}\,K^{-1}$) without bringing extra optical loss. Although the tuning speed of TOE (usually $10\sim100$ kHz) is much slower than that of FCE, it is usually enough for the reconfiguration of OADM and thus suitable for our proposed structure.

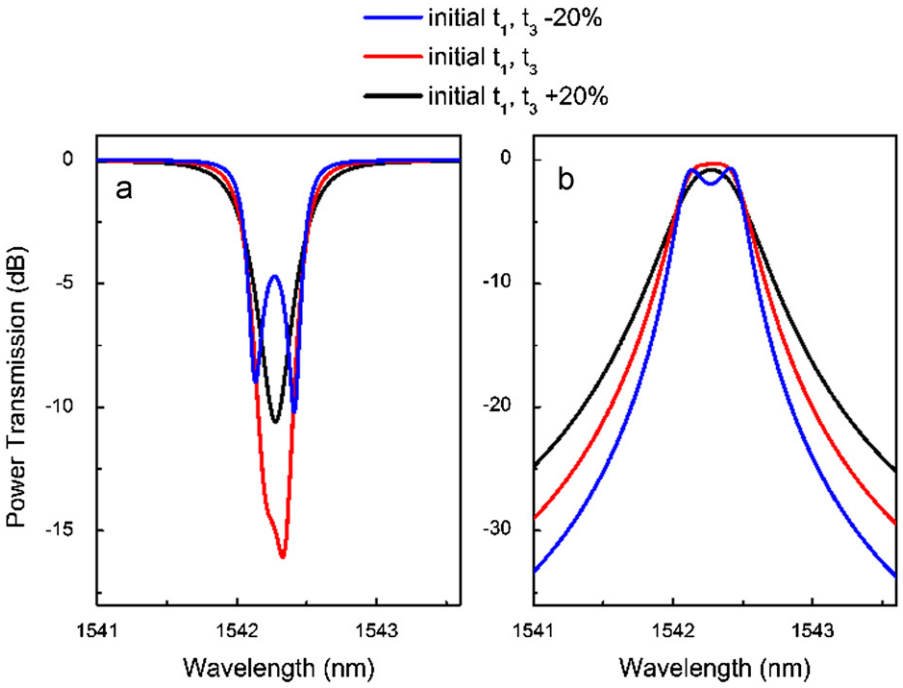

Fig. 6. (a) Through port and (b) drop port 1 spectra near channel 1 (λ=1542.3 nm) for different coupling coefficient t_1 and t_3.

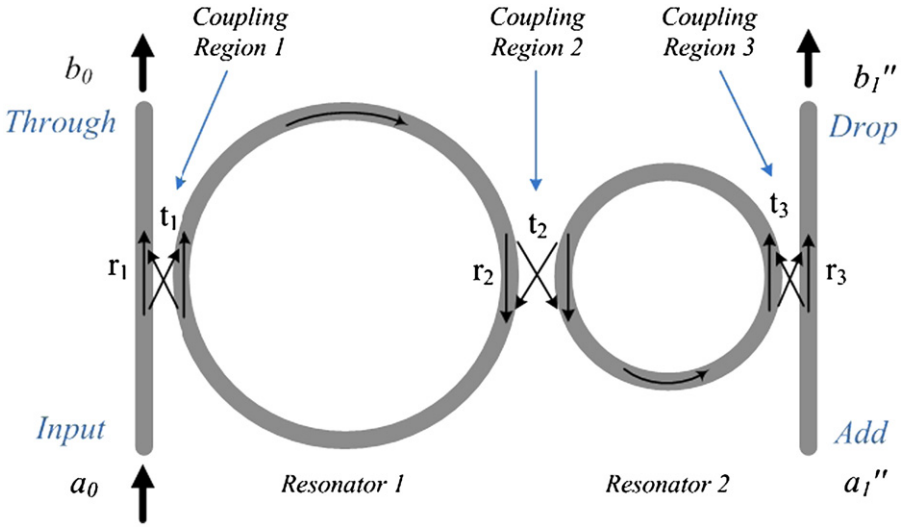

Fig. 7. Schematic of asymmetrical second-order series-coupled ring resonators.

The thermal crosstalk among the parent and sub rings should be considered when thermal tuning is applied to the sub-rings. The thermal crosstalk would make the resonances of the parent ring deviated from the original channel. For example, if the temperature change in the sub-rings is 100 K and there is a 10% thermal crosstalk, it would cause 10 K temperature change in the parent ring. Then there would be a redshift of 0.8 nm for the resonances of the parent ring. Thus, for a practical device, it is essential to introduce some electronic feedback system to stabilize the channel wavelengths or adopt specially designed heater pattern and isolation trenches to suppress thermal crosstalk as reported in [18,19].

For different applications, the passband bandwidth and channel crosstalk requirement may be different. Our simulation indicates that both the bandwidth and crosstalk could be varied by changing the coupling coefficients while maintaining the optimum condition to ensure flat passband. Fig. 5 shows the bandwidth and crosstalk at drop port 1 with varied coupling coefficients (Other parameters are the same as in Fig. 3). With the coupling coefficient t_2 varied from 0.2066 to 0.0675, the 3-dB bandwidth narrows from 0.63 to 0.17 nm. Meanwhile, the adjacent and non-adjacent channel crosstalk reduces by about 12 dB. This result indicates that there is a tradeoff between a broader bandwidth and a lower crosstalk, which is limited by the order of series-coupled ring resonator structure. To break through the limit, high-order series-coupled microrings could be used to replace the sub-ring, thus third or higher order resonators could be constructed with the parent ring. Higher order resonators would be helpful to improve passband characteristics and larger out-of-band rejection [4].

For a practical device, the propagation loss of Si waveguides may be fluctuated and the coupling coefficients may be deviated from the designed value due to fabrication errors. In order to investigate such impact, further simulations are carried out.

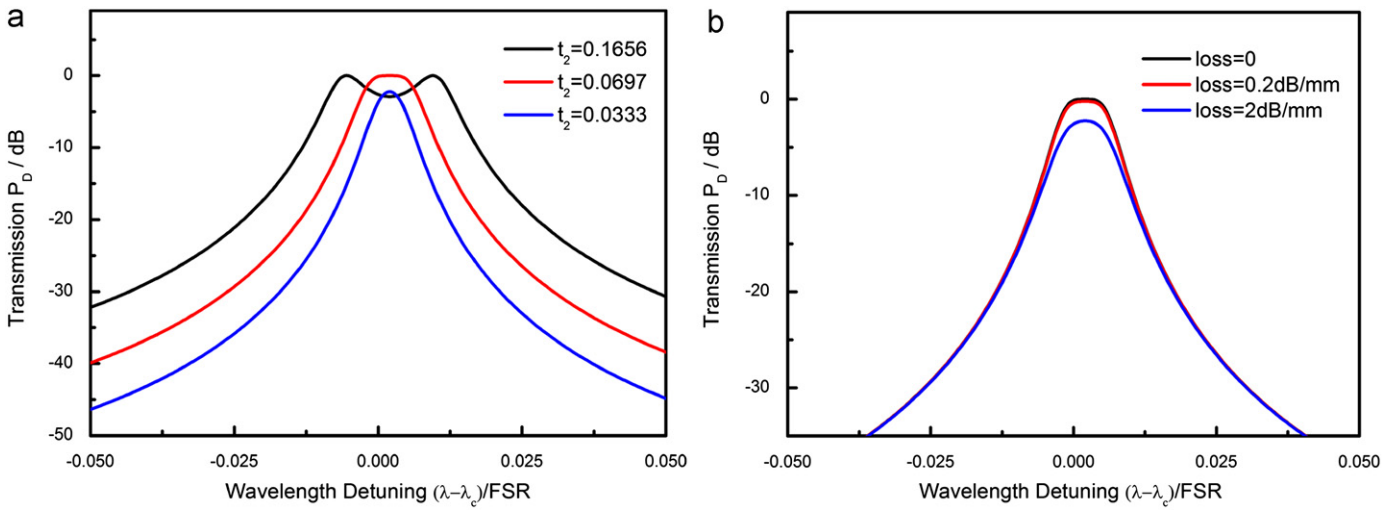

Fig. 8. Drop port spectra for (a) different coupling coefficient t_2 and (b) different propagation loss.

Firstly, the impact of waveguide loss is considered. In our proposed structure, the radius of the ring is large enough so that the bending loss is trivial. We consider typical propagation loss from 0.2 to 2 dB/mm (Other parameters are the same as in Fig. 3) and the results for drop port 1 are shown in Table 1. The deterioration of through port extinction and drop port transmission are only $\sim$2 dB. Meanwhile, the bandwidth and channel crosstalk are nearly unchanged. Secondly, we also calculate the performance of OADM involving the variation of the coupling coefficients. We assume that there is a $\pm$20% fabrication error of the gaps in coupling region #1 and #3 simultaneously, which introduces $\sim\pm$20% change of t_1 and t_3 from the initial values (t_1=0.4931, t_2=0.1515, t_3=0.4654, same as in Fig. 3) with fixed t_2. Since the optimum condition is no longer satisfied, the responses of both through and dropt port deteriorate (see Fig. 6). The through port extinction would be less than $-$10 dB whereas the ripples in the passband is $\sim$1 dB deep. The influence for other parameters such as the bandwidth and channel crosstalk is not significant. These results indicate that our proposed structure is relatively robust to the fluctuation in fabrication.

4. Conclusion

A parent-sub ring structure is designed for the application of OADM. Extended FSR without introducing significant bending loss, nearly uniform channel spacing and small footprint suitable for high-density integration are obtained through this design. The power transmission of the OADM is deduced by transfer matrix method and the transmission spectrum of a four-channel OADM is calculated. Here, in order to demonstrate the principle more clearly, only a simple case of the proposed structure is considered. Actually, the FSR of the OADM can be further extended by proper choice of ring radius and it is possible to reduce the channel crosstalk by using high-order ring resonators to replace the sub-rings. The proposed structure could also be extended to more channels by cascading in series or adding more sub-rings.

Acknowledgments

The authors would like to thank Dr. W. Zhang, Dr. K.Y. Cui, Dr. Q. Zhou and Dr. Q. Zhao for their valuable discussions and helpful comments. This work was supported by the National Basic Research Program of China (No. 2011CBA00608, 2011CBA00303, 2011CB301803, and 2010CB327405), the National Natural Science Foundation of China (Grant nos. 61036011 and 61036010), and the Project of Science and Technology on Communication Information Security Control Laboratory.

Appendix

Fig. 7 is the schematic of an asymmetrical second-order series-coupled ring resonator. The field amplitudes at the four ports are denoted as a_0, b_0, a_1'' and b_1'' while the field self- and cross-coupling coefficients in the three coupling regions are denoted as r_m and t_m (m=1, 2, 3) with the relation of $|r_m|^2+|t_m|^2=1$ for lossless coupling. Unlike in [20], we consider the case that the circumferences of the two rings (L_1 and L_2) are different, so the coupling in region 1 and 3 maybe different, i.e. $r_1\neq r_3$ (or $t_1\neq t_3$).

With transfer matrix method, the relationship among field amplitudes at the four ports could be expressed as:

$$\begin{pmatrix} a_1'' \\ b_1'' \end{pmatrix} = P_3Q_2P_2Q_1P_1\begin{pmatrix} a_0 \\ b_0 \end{pmatrix} \tag{1}$$

In Eq. (1), P_m (m=1, 2, 3) and Q_n (n=1, 2) are 2 by 2 transfer matrices that characterize the three coupling regions and field propagation in the two rings, respectively:

$$P_m=\frac{i}{t_m}\begin{bmatrix} -r_m & 1 \\ -1 & r_m \end{bmatrix},\quad Q_n=\begin{bmatrix} 0 & \sqrt{\mu_n}e^{-i\theta_n/2} \\ \left(\sqrt{\mu_n}e^{-i\theta_n/2}\right)^{-1} & 0 \end{bmatrix}$$

where μ_n represents the single-round amplitude transmission and $\theta_n=\beta L_n$ represents the single-round phase shift. Here, the propagation constants of all waveguides are treated as equal β. To simplify the calculation, we neglect the propagation loss, that is $\mu_1\approx\mu_2\approx 1$.

Consider zero input at the add port, $a_1''=0$, then the power transmission at the drop port could be deduced as:

$$T_{drop}=\left|\frac{b_1''}{a_0}\right|^2=\frac{p}{q} \tag{2}$$

where:

$$p=t_1^2t_2^2t_3^2$$

$$q=1+r_1^2r_2^2+r_2^2r_3^2+r_3^2r_1^2-2r_1r_2(1+r_3^2)\cos\theta_1-2r_2r_3(1+r_1^2)\cos\theta_2 +2r_1r_3(\cos(\theta_1+\theta_2)+r_2^2\cos(\theta_1-\theta_2))$$

In order to acquire maximally flat peak in the drop port spectrum, the second-order derivative of T_{drop} with respect to β should be equal to zero at resonant wavelength (where both βL_1 and βL_2 are multiples of 2π). Then we can obtain the following relation, i.e., the optimum condition:

$$r_2 = g \pm \sqrt{g^2 - h^2} (0 < r_2 < 1) \tag{3}$$

where:

$$g = \frac{r_1(1+r_3^2) + r_3(1+r_1^2)(L_2/L_1)^2}{2r_1 r_3 (1 - L_2/L_1)^2}$$

$$h = \frac{1+L_2/L_1}{1-L_2/L_1}$$

Comparing with the results in [17], the optimum condition for the asymmetrical configuration here includes an extra factor – the ratio of the two rings' circumference L_2/L_1.

Fig. 8(a) shows the transmission spectrum around resonant wavelength in the case of $L_2/L_1=2/5$, $r_1=0.8937$,$r_3=0.9570$ (or $t_1=0.4486$, $t_3=0.2900$) while the propagation loss is considered to be negligible. According to (3), the optimum r_2 is equal to 0.9976 ($t_2=0.0697$). When r_2 deviates from the optimum condition, the drop port spectrum will split into two peaks or have larger insertion loss.

To evaluate the influence of propagation loss to the above optimum condition, we set the loss as 0.2 dB/mm (a typical value in most of the simulations in this paper) and much larger value of 2 dB/mm and calculate the spectrum. The result in Fig. 8(b) shows that the spectra with/without loss are very close. Even for loss of 2 dB/mm, the deviation is still not significant. Therefore, the optimum condition without propagation loss is valid for a practical lossy waveguide with typical loss of 0.2 dB/mm.

References

[1] D.A.B. Miller, Proceedings of the IEEE 88 (2000) 728.
[2] R. Soref, IEEE Journal of Selected Topics in Quantum Electronics 12 (2006) 1678.
[3] X. Zheng, I. Shubin, G. Li, T. Pinguet, A. Mekis, J. Yao, H. Thacker, Y. Luo, J. Costa, K. Raj, J.E. Cunningham, A.V. Krishnamoorthy, Optics Express 18 (2010) 5151.
[4] B.E. Little, S.T. Chu, H.A. Haus, J. Foresi, J.P. Laine, Journal of Lightwave Technology 15 (1997) 998.
[5] S.T. Chu, B.E. Little, W.G. Pan, T. Kaneko, S. Sato, Y. Kokubun, IEEE Photonics Technology Letters 11 (1999) 691.
[6] M.A. Popovic, T. Barwicz, M.R. Watts, P.T. Rakich, L. Socci, E.P. Ippen, F.X. Kaertner, H.I. Smith, Optics Letters 31 (2006) 2571.
[7] S.J. Xiao, M.H. Khan, H. Shen, M.H. Qi, Optics Express 15 (2007) 14765.
[8] X. Shijun, M.H. Khan, S. Hao, Q. Minghao, Journal of Lightwave Technology 26 (2008) 228.
[9] A.M. Prabhu, A. Tsay, Z. Han, V. Van, IEEE Photonics Technology Letters 21 (2009) 651.
[10] X. Qianfan, D. Fattal, R.G. Beausoleil, Optics Express 16 (2008) 4309.
[11] Y. Yanagase, S. Suzuki, Y. Kokubun, S.T. Chu, Journal of Lightwave Technology 20 (2002) 1525.
[12] B. Timotijevic, G. Mashanovich, A. Michaeli, O. Cohen, V.M.N. Passaro, J. Crnjanski, G.T. Reed, Chinese Optics Letters 7 (2009) 291.
[13] R. Boeck, N.A.F. Jaeger, N. Rouger, L. Chrostowski, Optics Express 18 (2010) 25151.
[14] J. Garcia, A. Martinez, J. Marti, Optics Communications 282 (2009) 1771.
[15] J. Heebner, R. Grover, T. Ibrahim, Optical Microresonators: Theory, Fabrication, and Applications Introduction, Springer, London, 2008.
[16] J.K.S. Poon, J. Scheuer, Y. Xu, A. Yariv, Journal of the Optical Society of America B 21 (2004) 1665.
[17] R.A. Soref, B.R. Bennett, IEEE Journal of Quantum Electronics 23 (1987) 123.
[18] P. Dong, W. Qian, H. Liang, R. Shafiiha, N.N. Feng, D.Z. Feng, X.Z. Zheng, A.V. Krishnamoorthy, M. Asghari, Optics Express 18 (2010) 9852.
[19] H. Ting, W. Wanjun, Q. Chen, Y. Ping, Q. Huiye, Z. Yong, J. Xiaoqing, Y. Jianyi, IEEE Photonics Technology Letters 24 (2012) 524.
[20] T. Kato, Y. Kokubun, Journal of Lightwave Technology 24 (2006) 991.